

Stereographic Rectification of Omnidirectional Stereo Pairs

Jan Heller

Tomáš Pajdla

Center for Machine Perception, Department of Cybernetics,
Faculty of Elec. Eng., Czech Technical University in Prague

{hellej1,pajdla}@cmp.felk.cvut.cz

Abstract

We present a general technique for rectification of a stereo pair acquired by a calibrated omnidirectional camera. Using this technique we formulate a new stereographic rectification method. Our rectification does not map epipolar curves onto lines as common rectification methods, but rather maps epipolar curves onto circles. We show that this rectification in a certain sense minimizes the distortion of the original omnidirectional images. We formulate the rectification for multiple images and show that the choice of the optimal projection center of the rectification is under certain circumstances equivalent to the classical problem of spherical minimax location. We demonstrate the behaviour and the quality of the rectification in real experiments with images from 180 degree field of view fish eye lenses.

1. Motivation

A pair of images is thought to be rectified when its epipolar lines coincide. Rectification is typically a pre-step for methods of dense stereo matching and is mostly parameterized so that epipolar lines coincide with image scanlines. This type of rectification simplifies the following dense stereo matching and various methods for scanline rectification with respect to minimization of image distortion have been developed [8, 9, 7]. Although these methods perform well when epipoles are not present in the original images, they produce infinitely large images otherwise. Pollefeys *et al.* [12] proposed a rectification method based on polar parameterization, producing finite area images even when epipoles are located in the images.

However, in case of omnidirectional images epipolar lines become *epipolar curves*. Another difference between perspective and omnidirectional epipolar geometries is the existence of a *second epipole* in a single image. As the closest equivalent to the method described in [12], spherical parameterization can be considered. In [1], Arifan and Frossard used spherical parameterization in connection with

an energy minimization based approach to estimate dense disparities from omnidirectional images. In [6] Geyer and Daniilidis proved the existence of conformal rectification for stereo pairs obtained using a parabolic catadioptric camera, superposing bipolar coordinate system onto the two epipoles.

Nonetheless, both spherical and bipolar parameterizations inherit a significant setback congenital to all types of scanline rectifications – a severely disproportional expansion of the area near epipoles. Since at least one epipole is always present in an omnidirectional image, every scanline rectified omnidirectional image suffers from this blowout. This might not pose a problem in cases when rectified stereo pair is used as a pre-step for epipolar lines marching techniques, since the epipolar lines are parameterized anyway. However, it can be heavily counterproductive when techniques concerned with point neighbourhoods are employed.

In this paper we present a general method of rectification of a calibrated omnidirectional stereo pair and a novel rectification method based on the stereographic projection which we call the *stereographic rectification*. Using the stereographic projection, the scanline rectification is replaced by an epipolar curve rectification which maps circles on circles. In exchange for such a mapping we get a parameterization that in a certain sense minimizes distortion of original images as well as distances between corresponding image points. Besides that, circles are easy to parameterize and the length of a circle segment is easy to compute for further sampling optimization. Since the epipolar geometry is applied, the shapes of scanning windows for the same pixel positions are identical and distortion of the scanning window is governed by the geometry of circles. Further, the intersection of the respective fields of view (FOV) can be parameterized as intersection of two circles.

2. General rectification of stereo pairs

2.1. Geometry of omnidirectional cameras

By a *central omnidirectional camera* we understand any large view angle camera with a single effective viewpoint

and by *image formation* the formation of an image from a surrounding scene through an optical system to a digital camera's chip and the process of digitization. We assume that the cameras are calibrated and that the epipolar geometry of a stereo pair has been computed, *e.g.* by [10]. Geometry, calibration and the process of image formation of such central omnidirectional cameras are described in [3, 4, 5, 10, 11, 13].

The objective of the camera calibration is to find the mapping from an image point to a corresponding 3D ray represented by a unit vector. Formally, the camera calibration of a specific camera is a map $C : \mathbb{R}^2 \rightarrow \mathbb{S}^3$, where $\mathbb{S}^3 \stackrel{\text{def}}{=} \{\mathbf{v} \in \mathbb{R}^3 : \|\mathbf{v}\| = 1\}$. In this paper the availability of C and existence of inverse mapping C^{-1} is always assumed. Further, a canonical orientation such that $C((0,0))^T = (0,0,-1)^T$ is assumed.

2.2. Epipolar geometry

The central notion of the image rectification is *epipolar geometry* [8]. An analogy to the epipolar geometry of central perspective cameras can be formulated for central omnidirectional cameras likewise [10, 14]. The difference between directional and omnidirectional cameras is the shape of the retinas as well as the distinguishability of the ray orientations and thus existence of two epipoles. Here, we will use the spherical model of the retinas [10]. In the spherical model, intersections of epipolar planes and the retinas form pencils of epipolar circles. In the following, epipoles will be denoted $\mathbf{e}_{1,1}, \mathbf{e}_{1,2} \in \mathbb{S}^3$ for epipoles in the first view, $\mathbf{e}_{2,1}, \mathbf{e}_{2,2} \in \mathbb{S}^3$ for epipoles in the second view, $\mathbf{E} \in \mathbb{R}^{3 \times 3}$ will denote the essential matrix describing a particular epipolar geometry, $\mathbf{e}_{2,i} \mathbf{E} \mathbf{e}_{1,i} = 0$, $i = 1, 2$. Epipoles are oriented such that $\mathbf{e}_{1,1}, \mathbf{e}_{2,1}$ are always directions to the same scene point \mathbf{X} and such that if only one epipole is visible in the first view, $\mathbf{e}_{1,1}$ is that epipole. In the following we will use the following observation:

Observation 1 *Let \mathbf{E} be an essential matrix and $\mathbf{e}_{1,i}, \mathbf{e}_{2,i}$, $i = 1, 2$ the respective epipoles, $\mathbf{u} \in \mathbb{R}^3 \setminus \{(0,0,0)^T\}$ such that \mathbf{u} and $\mathbf{e}_{1,2}$ are linearly independent. Then vectors \mathbf{u} and $[\mathbf{e}_{2,2}]_{\times} \mathbf{E} \mathbf{u}$ lie in the same epipolar plane.*

2.3. Epipolar alignment

Given two calibrated images of the same rigid scene and an essential matrix describing the epipolar geometry of the image pair, the goal of this section is to derive transformation A_1 from the coordinate system of the first camera C_1 and transformation A_2 from the coordinate system of the second camera C_2 to the world coordinate system so the respective epipole pairs $\mathbf{e}_{1,i}, \mathbf{e}_{2,i}$, $i = 1, 2$ coincide with the z axis and the corresponding epipolar circles are superimposed, see Figure 1. The pair $[A_1, A_2]$ will be called the

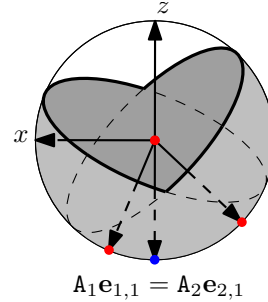


Figure 1. *Epipolar alignment example.* The Red dots denote camera centers and vectors incident to the respective centers of the fields of view. The blue dot represents the position of the epipoles after the epipolar alignment. The grey areas represent the vectors in the fields of view of the respective cameras.

epipolar alignment of an image pair. It is a simple observation that transformations $A_1, A_2 : \mathbb{R}^3 \rightarrow \mathbb{R}^3$ are linear invertible mappings expressed as matrix multiplications

$$\forall \mathbf{q} \in \mathbb{R}^3 : A_1(\mathbf{q}) = A_1 \mathbf{q}, A_2(\mathbf{q}) = A_2 \mathbf{q}, \quad (1)$$

where $A_1, A_2 \in \mathbb{R}^{3 \times 3}$ such that A_1 and A_2 map z axis of the world coordinate system onto the respective epipoles.

Definition 1 *Let \mathbf{e} be an epipole in an image from an omnidirectional stereo pair. We say that a coordinate system $\Sigma_{\mathbf{e}}^{\mathbf{u}} = [\mathbf{x}, \mathbf{y}, \mathbf{e}]$, so that $\mathbf{u} \in \mathbb{S}^3$ and \mathbf{e} are linearly independent, $\mathbf{x} = [\mathbf{e}]_{\times} \mathbf{u}$ and $\mathbf{y} = [\mathbf{x}]_{\times} \mathbf{e}$ is the epipolar coordinate system incident to the epipole \mathbf{e} with up-vector \mathbf{u} .*

Let \mathbf{E} be an essential matrix, $\mathbf{e}_{1,i}, \mathbf{e}_{2,i}$, $i = 1, 2$ the respective epipoles, as described in the previous section, $I = [(1,0,0)^T, (0,1,0)^T, (0,0,1)^T]$ the world coordinate system. Transformation from the ordered basis $\Sigma_{\mathbf{e}_{1,2}}^{\mathbf{u}_1}$ to the ordered basis I and transformation from the ordered basis $\Sigma_{\mathbf{e}_{2,2}}^{\mathbf{u}_2}$ to the ordered basis I , for $\mathbf{u}_1, \mathbf{u}_2 \in \mathbb{R}^3$, where \mathbf{u}_1 is not collinear with $\mathbf{e}_{1,2}$ and \mathbf{u}_2 is not collinear with $\mathbf{e}_{2,2}$, would solve the goal of superimposing epipoles with z axis. However, in order to superimpose epipolar circles as well, another constraint to these mappings must be introduced. In order to ensure superposition of epipolar circles, up-vectors $\mathbf{u}_1, \mathbf{u}_2$ have to “select” the same epipolar circle, *i.e.* lie in the same epipolar plane. It follows from Observation 1 that $\mathbf{u}_2 = [\mathbf{e}_{2,2}]_{\times} \mathbf{E} \mathbf{u}_1$ is a sufficient condition for $\mathbf{u}_1, \mathbf{u}_2$ to lie in the same epipolar plane.

Let us derive the epipolar transformation $[A_1, A_2]$. Since A_1^{-1} is the transformation from the ordered basis I to the ordered basis $\Sigma_{\mathbf{e}_{1,2}}^{\mathbf{u}_1} = [\mathbf{x}, \mathbf{y}, \mathbf{e}_{1,2}]$,

$$A_1^{-1} I = \Sigma_{\mathbf{e}_{1,2}}^{\mathbf{u}_1}, \quad (2)$$

$$A_1 = (\mathbf{x} \quad \mathbf{y} \quad \mathbf{e}_{1,2})^{-1}. \quad (3)$$

Observation 2 Let $\mathbf{R} \in \mathbb{R}^{3 \times 3}$ be an orthogonal matrix, $\mathbf{N} = \mathbf{R}(0, 0, 1)^\top$. Then

$$\forall \mathbf{q} \in \mathbb{S}^3 : S_{\mathbf{N}}(\mathbf{q}) = S(\mathbf{R}^{-1}\mathbf{q}). \quad (10)$$

4. Stereographic rectification

In this paper we propose a novel rectification method we call the *stereographic rectification* to address the issue of epipole expansion of previous rectification methods, *e.g.* [1, 6]. For this reason we chose the stereographic projection as its characteristic transformation. The stereographic projection maps epipoles onto points instead of lines, as is the inherent case of previous rectification methods. Because of this the stereographic rectification does not map epipolar curves onto scanlines but onto general circles. However, there is a setback to the stereographic projection – as any sphere to plane conformal map it does not preserve area. Along the unit circle, there is no distortion of area but near infinity areas are distorted by arbitrarily large factors. It can be shown that the ratio of an area element and its projection under the stereographic projection depends only on the distance of the area element from the center of the projection on the unit sphere. This leads to an intuitive observation that to minimize the distortion one could minimize the maximal ratio for an area element from Ω . Since both Ω and stereographic projection are given, one can change only the position of the projection center \mathbf{N} to change the position and thus the distortion of $S_{\mathbf{N}}(\Omega)$. We chose to formulate this observation to quantify what we call the *optimal projection center* for an area Ω as

$$\mathbf{N} = \arg \max_{\mathbf{p} \in \mathbb{S}^3} \Delta(\Omega, \mathbf{p}), \quad (11)$$

where Δ is the spherical distance between \mathbf{p} and Ω ,

$$\Delta(\Omega, \mathbf{p}) \stackrel{\text{def}}{=} \inf_{\mathbf{q} \in \Omega} \arccos(\mathbf{p}^\top \mathbf{q}). \quad (12)$$

If more areas of interest are considered, a compromise in distortions introduced to the respective areas can be achieved by projecting from a point maximizing the distance from the union of the areas,

$$\mathbf{N} = \arg \max_{\mathbf{p} \in \mathbb{S}^3} \Delta\left(\bigcup_{i \in I} \Omega_i, \mathbf{p}\right), \quad (13)$$

where $I = \{1, \dots, n\}$ and n is the number of the studied areas.

In the case of the stereographic rectification the areas of interest are the respective fields on view. If we denote $V_i \subset \mathbb{R}^2, i \in I$ as sets of pixels lying in the fields of view of the respective images, *i.e.* the FOV ellipses, the “visible”

directions in the coordinate systems of the respective cameras form

$$\Omega'_i = \{\mathbf{p}' : \mathbf{p}' \in \mathbb{S}^2 \ \& \ C_i^{-1}(\mathbf{p}') \in V_i\}, \quad (14)$$

where C_i are respective calibration transformations. After the epipolar alignment, Ω'_i transform to

$$\Omega_i = \{\mathbf{p} : \mathbf{p} \in \mathbb{S}^3 \ \& \ C_i^{-1}(\mathbf{A}_i^{-1}\mathbf{p}) \in V_i\}. \quad (15)$$

Now the characteristic transformation of the stereographic rectification T_{SGR} can be formulated:

$$\forall \mathbf{q} \in \mathbb{R}^3 : T_{SGR}(\mathbf{q}) = S_{\mathbf{N}}(\mathbf{q}). \quad (16)$$

Using Observation 2 we can express the inverse characteristic transformation of the stereographic rectification

$$\forall \mathbf{u} \in \mathbb{R}^2 : T_{SGR}^{-1}(\mathbf{u}) = \mathbf{R}S^{-1}(\mathbf{u}), \quad (17)$$

where $\mathbf{R} \in \mathbb{R}^{3 \times 3}$ is an orthogonal matrix such that $\mathbf{R}(0, 0, 1)^\top = \mathbf{N}$. Any such \mathbf{R} can express the change of the projection center to \mathbf{N} , affecting only rotation of the resulting 2D image. We choose $\mathbf{R} = \begin{pmatrix} \mathbf{r}_1 & \mathbf{r}_2 & \mathbf{N} \end{pmatrix}$ such that $\mathbf{r}_1 = [(0, 1, 0)^\top]_{\times} \mathbf{N}$, $\mathbf{r}_2 = [\mathbf{N}]_{\times} \mathbf{r}_1$.

To finalize the description of the stereographic rectification the final affine transformation needs to be specified. Here, we define final affine transformation F_{SGR} based on a parameter $a \in \mathbb{R}$, cropping the range of T_{SGR} to $[-a, a] \times [-a, a]$. The final affine transformation $F_{SGR} : \mathbb{R}^2 \rightarrow \mathbb{R}^2$ for an image with width w and height h reads as

$$\forall \mathbf{u} \in \mathbb{R}^2 : F_{SGR}(\mathbf{u}) = \begin{pmatrix} \frac{w}{2a} & 0 \\ 0 & \frac{h}{2a} \end{pmatrix} \mathbf{u} + \begin{pmatrix} \frac{w}{2} \\ \frac{h}{2} \end{pmatrix}. \quad (18)$$

F_{SGR}^{-1} can be derived trivially.

4.1. Two view stereographic rectification

Although Equation 16 is a mathematically correct definition of a transformation, it says a little about its actual enumeration. The obstacle lies in the computation of the optimal projection center \mathbf{N} , which in its general formulation and with general shapes of Ω_i poses a rather difficult optimization problem. However, we can heavily simplify this by assuming that the FOVs of both cameras is 180° ¹. Then $\Omega'_i, i = 1, 2$ become exactly the southern hemisphere $\Omega'_i = \{\mathbf{p} : \mathbf{p} \in \mathbb{S}^3 \ \& \ \mathbf{N}'_i{}^{-1}\mathbf{p} \leq 0\}$, where $\mathbf{N}'_i = (0, 0, 1)^\top$ are the hemisphere “normals”. After the epipolar alignment $\Omega'_i, i = 1, 2$ transform into arbitrary positioned hemispheres $\Omega_i = \{\mathbf{p} : \mathbf{p} \in \mathbb{S}^3 \ \& \ \mathbf{N}_i^\top \mathbf{p} \leq 0\}$, where $\mathbf{N}_i = \mathbf{A}_i(0, 0, 1)^\top$ are the new normals, see Figure 3. Using these constraints, Theorem 1 explicitly states the optimal projection center.

¹The 180° assumption can be relaxed to a radially symmetric FOV with the same results.

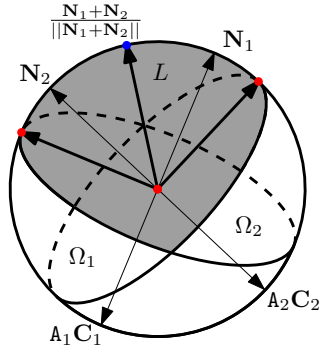


Figure 3. *Optimal projection vector.* Example of the epipolar alignment of two fields of view of 180° $\Omega_i, i = 1, 2$ and the resulting optimal projection center of the stereographic rectification.

Theorem 1 Let $i = 1, 2$, A_i be the epipolar alignment of a stereo pair; $\mathbf{N}_i = A_i(0, 0, 1)^\top, \Omega_i = \{\mathbf{p} : \mathbf{p} \in \mathbb{S}^3 \ \& \ \mathbf{N}_i^\top \mathbf{p} \leq 0\}$. Then

$$\mathbf{N} = \arg \max_{\mathbf{v} \in \mathbb{S}^3} \Delta\left(\bigcup_{i \in \{1, 2\}} \Omega_i, \mathbf{v}\right) = \frac{\mathbf{N}_1 + \mathbf{N}_2}{\|\mathbf{N}_1 + \mathbf{N}_2\|}. \quad (19)$$

4.2. Multiview stereographic rectification

Stereographic rectification can be also used to rectify more than two images. Such a rectification is useful if epipoles appear in images in similar locations, which happens when a camera travels along a line or a slowly varying curve. An extension of the general rectification technique presented in this paper for multiple images can be done by pairwise application of the respective epipolar constraints and by adaptation of the epipolar alignment so that the epipoles are not necessarily aligned with the z axis.

In this section we reformulate Equation 13 as the spherical minimax location problem. The spherical minimax location problem is a well known type of a minimax problem and can be solved in polynomial time, *e.g.* using an algorithm by Das *et al.* [2].

Let's assume that the visible angle of n cameras is 180° , $\Omega_i, i \in I = \{1, \dots, n\}$ are the hemispheres after epipolar alignment and \mathbf{N}_i are the hemispheres "normals". Since $\Delta(\bigcup_{i \in I} \Omega_i, \mathbf{p}) = \Delta(\Omega_j, \mathbf{p})$ for a certain $j \in I$, the union operation and the distance operators in Equation 13 can be swapped to get

$$\mathbf{N} = \arg \max_{\mathbf{p} \in \mathbb{S}^3} \min_{i \in I} \Delta(\Omega_i, \mathbf{p}). \quad (20)$$

Further, using the assumption that Ω_i are hemispheres, the minimization of the distances of \mathbf{p} to Ω_i can be expressed as the maximization of the spherical distance of \mathbf{p} and the hemisphere normals \mathbf{N}_i

$$\mathbf{N} = \arg \max_{\mathbf{p} \in \mathbb{S}^3} \left(\frac{\pi}{2} - \max_{i \in I} \delta(\mathbf{N}_i, \mathbf{p}) \right), \quad (21)$$

where

$$\delta(\mathbf{p}, \mathbf{q}) \stackrel{\text{def}}{=} \arccos(\mathbf{p}^\top \mathbf{q}). \quad (22)$$

Finally, since addition of a constant is identity under $\arg \max$ operation and the fact that $\max(-f(x)) = \min(f(x))$, we get

$$\mathbf{N} = \arg \min_{\mathbf{p} \in \mathbb{S}^3} \max_{i \in I} \delta(\mathbf{N}_i, \mathbf{p}). \quad (23)$$

The resulting Equation 23 is the direct formularization of the spherical minimax location problem. Theorem 1 is a direct consequence of Equation 23, see Figure 3.

5. Experiments

For experimentation with stereo pairs we implemented the stereographic rectification and several other pre-existing methods in MATLAB. The code is available for download at <http://cmp.felk.cvut.cz/~pajdla/software/omnirect/omnirect-1.0.2.tar.bz2>.

'Street' sequence, see Figure 4, was acquired using Canon EOS 1Ds with Sigma 8mm-f4-EX fish-eye lens. An image pair further referred to as P_L , Figure 4(a,b), resulted from a lateral move of the camera between the shots. An image pair further referred to as P_F , Figure 4(d,e), resulted from a forward move of the camera between the shots. Images were transformed to appear as if they were acquired by a para-catadioptric camera in order to transform epipolar curves into circles. Several epipolar curves are shown in the pictures, as well as projections $\mathbf{u}_{e_{i,j}}, i, j = 1, 2$ of the respective epipoles $e_{i,j}$. Figure 4(c) shows the overlay of P_L with Figure 4(a) in the red channel and Figure 4(b) in the green channel. Figure 4(f) shows the overlay of P_F with Figure 4(d) in the red channel and Figure 4(e) in the green channel.

Scanline rectification methods [1, 6] perform reasonably well in the case of the lateral move in P_L , see Figures 4(g) for the overlay of the rectification based on spherical parameterization [1], 4(h) for the overlay of the rectification based on bipolar parameterization [6]. Yet there is a noticeable area enlargement around epipoles in both cases. However, the scanline rectification methods produce heavily distorted images in the case of the forward move in P_F , see Figures 4(j) for the overlay of the rectification based on spherical parameterization [1], 4(k) for the overlay of the rectification based on bipolar parameterization [6]. Again, in the case of the scanline rectification methods the areas near the epipoles are heavily expanded at the expense of the rest of the image. On the other hand, the stereographic rectification performs well for both the lateral and the forward move, see the rectification overlays in Figure 4(i) for

P_L and Figure 4(l) for P_F – the images produced using the stereographic rectification feature the least distortion compared to the original images. Both Figures 4(i) and 4(l) were produced using the parameter a from Equation 18 set to 1.2 and the free parameter of the epipolar alignment $u_1 = (0, 1, 0)^T$.

‘Office’ sequence, see Figure 5, was acquired using KYOCERA Finecam M410R with custom mounted Nikon FC-E8 fish-eye lens. It documents the behaviour of the stereographic rectification method in cases when an epipole is present between the center of the FOV and its boundary. The image pair P_{O_1} (Figures 5(a, b)) resulted from moving the camera along $\frac{1}{4}$ of a circle of diameter of about 2 m with the camera facing the center of the circle. The image pair P_{O_2} (Figures 5(d, e)) resulted from moving the camera along $\frac{1}{8}$ of the circle. Projections $\mathbf{u}_{e_{1,2}}$, $\mathbf{u}_{e_{2,1}}$ of the respective epipoles $e_{1,2}$, $e_{2,1}$ are shown in both pairs. Figure 5(c) shows the overlay of P_{O_1} with Figure 5(a) in the red channel and Figure 5(b) in the green channel. Figure 5(f) shows the overlay of P_{O_2} with Figure 5(d) in the red channel and Figure 5(e) in the green channel. Note that Figures 5(a) and 5(d) depict the same image.

In case of images with the 180° FOV, there is always at least one epipole visible in the FOV. The closer the epipole is to the center of the FOV, the greater distortion is introduced by a scanline rectification method, see Figure 5(g) for the overlay of the rectification of P_{O_1} based on spherical parameterization [1] and Figure 5(j) for the overlay of the rectification of P_{O_2} with the same type of rectification.

The stereographic rectification produces noticeable distortion as well, see Figure 5(h) for the rectification of P_{O_1} with a from Equation 18 set to 1, Figure 5(k) for the rectification of P_{O_1} with $a = 2.7$, Figure 5(i) for the rectification of P_{O_2} with $a = 1$, Figure 5(l) for the rectification of P_{O_2} with $a = 2.7$; $\mathbf{u}_1 = (0, 1, 0)^T$ for all Figures 5(h,k,i,l). However, as expected, the overlapping areas of the rectified images are mainly unaffected. The area expansion produced by the stereographic rectification, see Figure 5(k, l), is limited to the parts of the respective fields of view that do not overlap and thus poses no problem for stereo matching.

6. Conclusion

We presented a novel method for rectification of an omnidirectional stereo pair based on the stereographic projection. We formulated the stereographic rectification for multiple images as well. We showed that the choice of the optimal projection center of the stereographic rectification is for 180° FOV cameras equivalent to the classical spherical minimax location problem. This allowed us to provide an explicit formula for the optimal projection center of the stereographic rectification for the case of omnidirectional stereo pairs taken with 180° FOV lenses. We compared the stereographic rectification to previous rectification methods

and for several significant epipole positions showed that the stereographic rectification produces significantly less distorted images.

Acknowledgements

This work was supported by EC project FP7-SPA-218814 PRoVisG and Czech Government under the research program MSM6840770038.

References

- [1] Z. Arican and P. Frossard. Dense disparity estimation from omnidirectional images. In *2007 IEEE AVSS*, 2007.
- [2] P. Das, N. R. Chakraborti, and P. K. Chaudhuri. Spherical minimax location problem. *Computational Optimization and Applications*, 18(3):311–326, 2001.
- [3] C. Geyer and K. Daniilidis. A unifying theory for central panoramic systems and practical applications. *ECCV*, pages 445–461, 2000.
- [4] C. Geyer and K. Daniilidis. Catadioptric projective geometry. *IJCV*, 45:223–243, 2001.
- [5] C. Geyer and K. Daniilidis. Paracatadioptric camera calibration. *PAMI*, 24(5):687–695, 2002.
- [6] C. Geyer and K. Daniilidis. Conformal rectification of omnidirectional stereo pairs. *Omnivis*, June 2003.
- [7] J. Gluckman and S. Nayar. Rectifying transformations that minimize resampling effects. In *CVPR*, pages I:111–117, 2001.
- [8] R. Hartley and A. Zisserman. *Multiple view geometry in computer vision*. Cambridge University, Cambridge, 2nd edition, 2003.
- [9] C. Loop and Z. Zhang. Computing rectifying homographies for stereo vision. In *CVPR*, page I:1125, 1999.
- [10] B. Micusik and T. Pajdla. Structure from motion with wide circular field of view cameras. *PAMI*, 28(7):1135–1149, 2006.
- [11] S. K. Nayar. Catadioptric omnidirectional camera. *CVPR*, 0:482, 1997.
- [12] M. Pollefeys, R. Koch, and L. J. V. Gool. A simple and efficient rectification method for general motion. *ICCV*, pages 496–501, 1999.
- [13] H.-Y. Shum, A. Kalai, and S. M. Seitz. Omnivergent stereo. *ICCV*, 1:22, 1999.
- [14] T. Svoboda, T. Pajdla, and V. Hlaváč. Epipolar geometry of panoramic cameras. *ECCV*, pages 218–231, 1998.

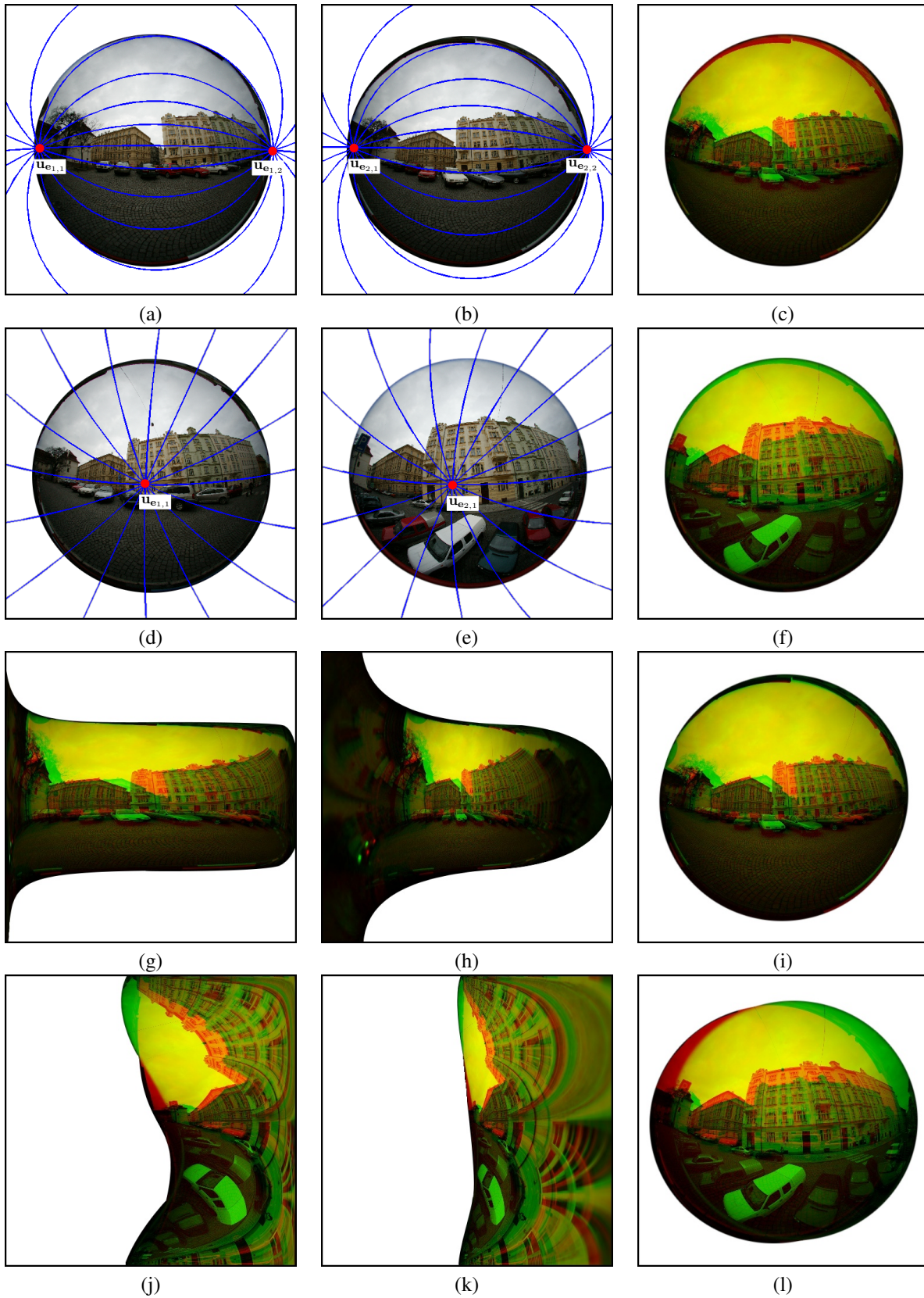


Figure 4. Comparison of previous rectification methods and the stereographic rectification, see text.

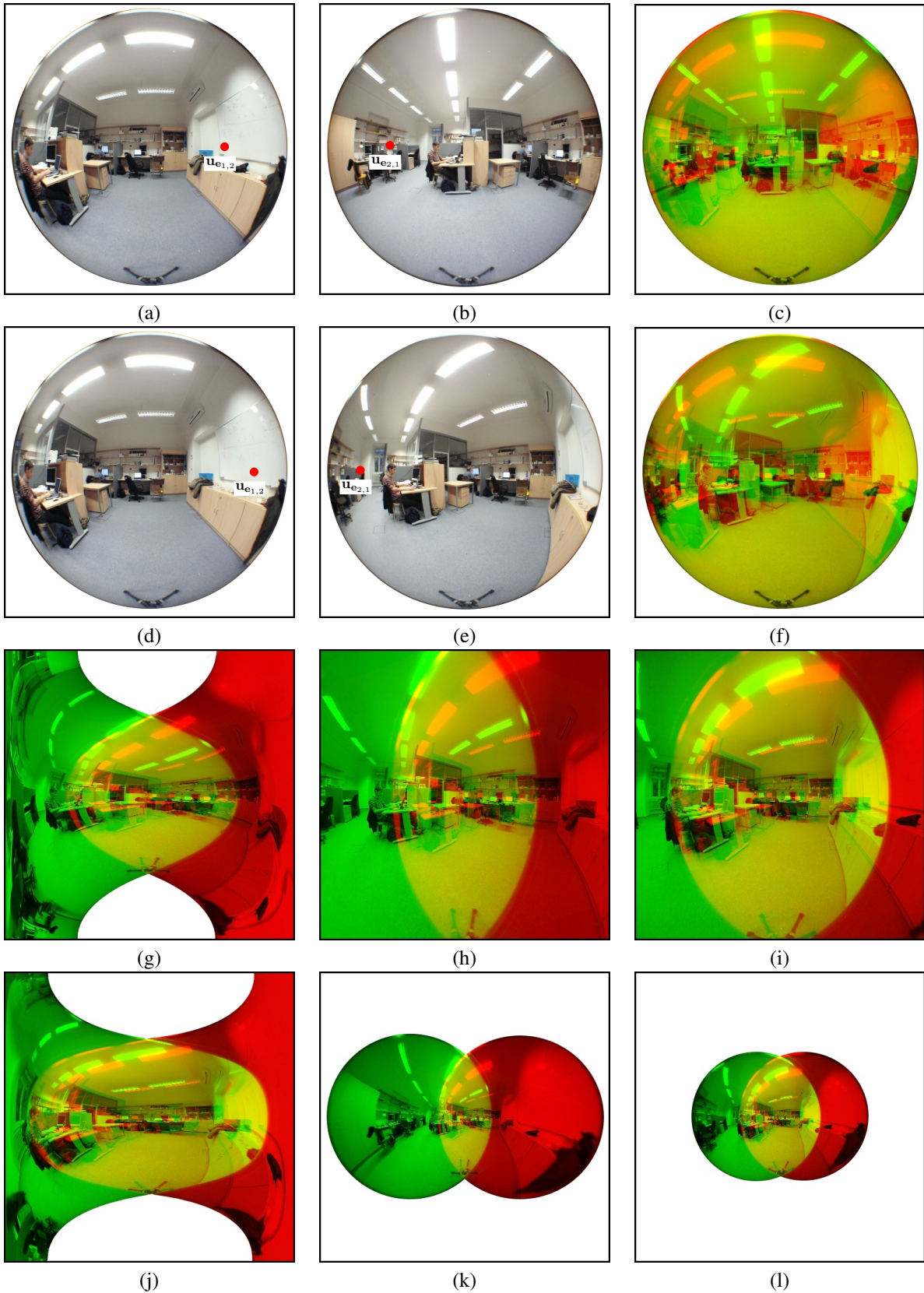


Figure 5. Comparison of previous rectification methods and the stereographic rectification, see text.